

9-20-2016

## Estimation of Raindrop Size Distribution Parameters Using Rain Attenuation Data from a Ku-Band Communications Satellite

Wira Indrayani

*Department of Physics, Faculty of Mathematics and Natural Science, Universitas Andalas, Padang 25163, Indonesia*

Marzuki

*Department of Physics, Faculty of Mathematics and Natural Science, Universitas Andalas, Padang 25163, Indonesia, marzuki@fmipa.unand.ac.id*

Mutya Vonnisa

*Department of Physics, Faculty of Mathematics and Natural Science, Universitas Andalas, Padang 25163, Indonesia*

Follow this and additional works at: <https://scholarhub.ui.ac.id/science>

---

### Recommended Citation

Indrayani, Wira; Marzuki; and Vonnisa, Mutya (2016) "Estimation of Raindrop Size Distribution Parameters Using Rain Attenuation Data from a Ku-Band Communications Satellite," *Makara Journal of Science*: Vol. 20 : Iss. 3 , Article 7.

DOI: 10.7454/mss.v20i3.6245

Available at: <https://scholarhub.ui.ac.id/science/vol20/iss3/7>

This Article is brought to you for free and open access by the Universitas Indonesia at UI Scholars Hub. It has been accepted for inclusion in Makara Journal of Science by an authorized editor of UI Scholars Hub.

---

# Estimation of Raindrop Size Distribution Parameters Using Rain Attenuation Data from a Ku-Band Communications Satellite

## Cover Page Footnote

The authors wish to thank Prof. Maekawa Yasuyuki and Prof. Yoshiaki Shibagaki (Osaka Electro-Communication University) for providing the data concerning the downlink radio wave signals of the Superbird-C satellite. We also wish to thank Dr. Hiroyuki Hashiguchi (Kyoto University), Dr. Toyoshi Shimomai, and Prof. Toshiaki Kozu (Shimane University) for their assistance in the collection and processing of the 2DVD and ORG data. The 2DVD and other Equatorial Atmospheric Radar (EAR) facilities at Koto Tabang are supported by GrantAid for Scientific Research on Priority Areas, which is funded by the Ministry of Education, Culture, Sports, Science, and Technology (MEXT) of Japan. This study is partially supported by the Faculty of Mathematics and Natural Science of Andalas University under Hibah Mandiri-2013.

## Estimation of Raindrop Size Distribution Parameters Using Rain Attenuation Data from a Ku-Band Communications Satellite

Wira Indrayani, Marzuki\*, and Mutya Vonnisa

Department of Physics, Faculty of Mathematics and Natural Science, Universitas Andalas, Padang 25163, Indonesia

\*E-mail: marzuki@fmipa.unand.ac.id

Received March 2, 2015 | Accepted January 25, 2016

---

### Abstract

The rain attenuation of down-link radio wave signals from the Superbird-C satellite and surface rainfall data have been used to estimate the parameters of exponential raindrop size distribution (DSD) at Koto Tabang (100.32 °E, 0.20 °S), West Sumatra, Indonesia. Prior to analyzing the measured data, the ability of the method to recover the parameters of known DSDs from which the samples were taken was examined. It was found that the method can accurately retrieve the input parameter of the sample. Only six case studies are presented here, so the results are representative rather than definitive. The method successfully estimated the DSD parameters of a stratiform case with steady intensity and deep convective rains of a short duration. This can be inferred from the small difference between the parameters derived from rain attenuation data and those derived from a 2D video disdrometer. The poor performance of the method was observed for a stratiform case with strong rain intensity fluctuation and shallow convective rains with very low rain top height. This phenomenon is probably due to the bias that may be inherent in the estimation of specific rain attenuation, such as the assumption of a constant path length throughout the rain.

### Abstrak

**Penentuan Parameter Distribusi Butiran Hujan dari Data Atenuasi Gelombang Elektromagnetik Satelit Telekomunikasi Berfrekuensi Ku-Band.** Data atenuasi sinyal *down-link* dari gelombang radio satelit Superbird C dan data curah hujan permukaan telah dimanfaatkan untuk menghitung parameter eksponensial distribusi butiran hujan (DSD) di Koto Tabang, Sumatera Barat, Indonesia. Pengujian metode terhadap data uji dengan parameter DSD yang diketahui menunjukkan bahwa metode ini dapat dengan akurat menghitung kembali parameter tersebut. Metode ini telah diujikan pada masing-masing dua studi kasus untuk hujan stratiform, *deep* dan *shallow* convective. Kemampuan metode ini untuk memperkirakan parameter DSD dari hujan *stratiform* dengan intensitas curah hujan yang stabil dan hujan *deep convective* dengan durasi singkat, sangat baik. Hal ini ditandai dengan kecilnya perbedaan antara parameter DSD yang berasal dari atenuasi hujan dan dari data *2D-Video disdrometer* (2DVD). Kurang baiknya kinerja metode ini teramati pada hujan *stratiform* dengan fluktuasi intensitas curah hujan yang besar dan dan hujan *shallow convective* dengan ketinggian puncak hujan yang sangat rendah. Fenomena ini kemungkinan disebabkan oleh bias dalam memperkirakan spesifik atenuasi seperti bias akibat asumsi panjang lintasan penjalaran yang konstan selama hujan.

*Keywords: rain attenuation, raindrop size distribution, electromagnetic wave, Sumatra*

---

### Introduction

The raindrop size distribution (DSD) is important due to its many applications, including cloud physics [1], weather radar data conversion [2,3], modeling of telecommunication systems, particularly for the microwave band [4,5], and the design of remote sensing systems for monitoring the atmosphere [6]. Given the importance of the DSD, there are many instruments available to directly measure the DSD, such as a disdrometer [7,8], Rain Occurrence Sensor System (POSS) [9], and micro rain radar [10]. In addition

to direct measurement, the DSD can also be indirectly retrieved from weather and atmospheric radar data because such data are a function of raindrop [11,12].

Rain causes attenuation in electromagnetic waves that degrades the system performance of communication [13] and weather radar [14]. The attenuation can increase path loss and limit the coverage area of microwave applications. It occurs through the absorption and scattering processes [15], and it increases with increasing rainfall rate and frequency. Rain attenuation is one of the most noticeable

components of excess losses, especially at frequencies above 10 GHz.

Besides the negative effects mentioned above, there are benefits to rain attenuation data. It can be used to estimate the DSD parameters because it is a function of raindrop properties, particularly the DSD. The DSD parameters can be indirectly obtained by combining the attenuation and other integral rainfall parameters (IRPs), such as rainfall rate or radar reflectivity factor. Manabe et al. [16] estimated the DSD parameters in Japan by combining rainfall rate and attenuation data from multifrequency observations at millimeter wave bands over the 1000 m line-of-sight link. Maitra and Gibbins [17] combined the rainfall rate and multiwavelength rain attenuation measurements at millimeter and infrared wave bands to estimate the DSD parameters at Chilbolton in Hampshire. Like [16], Maitra and Gibbins [17] also analyzed data from the line-of-sight link with a path length of 500 m. Therefore, both studies analyzed data from the line-of-sight link with a constant path length. In this paper, we examined the possibility of estimating the DSD parameters from attenuation data of a communications satellite in the Ku-band frequency. Unlike previous studies, the path length in this work is not constant, but rather it depends on the rain type. Another difference is that the current work analyzes data from a tropical region that receives a high amount of rainfall throughout the year.

## Methods

**Attenuation and rainfall rate data.** Rain attenuation data are available from the satellite links of the Superbird-C. The satellite connects the Research Institute for Sustainable Humanosphere (RISH) of Kyoto University in Japan to the Equatorial Atmosphere Radar (EAR) site at Koto Tabang, West Sumatera, Indonesia, with a data transmission rate of 128 kbps. At RISH, the carrier frequency of the up-link transmission is 14.1292 GHz, while it is 12.7351 GHz for the down-link. At EAR, on the other hand, the carrier frequency of the up-link transmission is 14.4651 GHz, while it is 12.3992 GHz for the down-link. A detailed description of the system can be found in [18]. For this work, we only have data from the down-link at Koto Tabang.

To estimate the DSD parameters, the rainfall rate and specific rain attenuation data are needed. The rainfall rate data are obtained from an optical rain gauge (ORG) measurement that samples the rain rate every 1 minute. Detailed specifications of this instrument can be found in [19]. The second variety of data concerns the specific rain attenuation, which is derived from the total attenuation of the down-link radio wave signals. The total attenuation is the product of specific attenuation  $\gamma$  (dB/km) and the propagation path length  $L$  (km), which is given by

$$A = \gamma L \quad (1)$$

The value of  $L$  is dependent on the rain type. For this study, we selected six rain events that have been classified according to their rain type and path length [20]. The rain events were classified into either the stratiform, mixed stratiform/convective, deep convective, or shallow convective type by analyzing the vertical structure of reflectivity, velocity, and spectral width derived from measurements made with the vertical beam of a 1.3 GHz wind profiler [21]. Table 1 summarizes the statistics of the selected rain events. The path length of each rain type was derived using the International Telecommunication Union Radiocommunication Sector (ITU-R) and the Simple Attenuation Model (SAM) [20].

**Integral rainfall parameters (IRPs) modeling.** As mentioned in the introduction, all IRPs are a function of the DSD. In this work, the DSD is modeled by a modified exponential distribution given by [22]

$$N(D) = N_0 e^{-\lambda D} \quad (2)$$

where  $D$  is the drop diameter and  $N_0$  and  $\lambda$  are the intercept and slope, respectively. The rainfall rate (mm/h) is expressed in terms of the DSD as

$$N(D) = 6 \times 10^{-4} \pi \int_0^{D_{\max}} v(D) D^3 N(D) dD \quad (3)$$

where  $v$  is the raindrop falling velocity (m/s), which is given by [23]

$$v(D) = 9.65 - 10.3 e^{(-0.6D)} \quad (4)$$

Finally, the specific rain attenuation is expressed in terms of the DSD as [4, 13, 16-17]

$$\gamma [dB/km] = 4.343 \times 10^3 \int_0^{D_{\max}} \sigma_{ext}(D, n, \lambda) N(D) dD \quad (5)$$

where  $\sigma_{ext}$  is the extinction cross section ( $m^2$ ) of the water sphere as a function of  $D$ , wavelength ( $\lambda$ ), and the refractive index of water. The complex refractive indices are obtained from the model of Liebe et al. [24] using the mean temperature during the rain event, which is measured by the ORG (Table 1). The extinction cross sections are derived from the efficiencies for extinction ( $Q_{ext}$ ) of Mie theory, which is given by:

$$Q_{ext} = \frac{2}{x^2} \sum_{n=1}^{\alpha} (2n+1) \text{Re}(a_n + b_n) \quad (6)$$

Where  $a_n$  and  $b_n$  are the Mie scattering coefficient and  $x$  is the parameter size ( $x = ka$ ), with  $a$  being the radius of the drop. The extinction cross section is related to the efficiencies for extinction as  $\sigma_{ext} = Q_{ext} \cdot \pi a^2$ . The

extinction cross section of raindrops assumed to be spherical is deduced from [15].

$$r = \frac{\gamma}{R} \tag{7}$$

**DSD parameter estimation.** The  $N_0$  and  $\Lambda$  in equation (2) are estimated by following the method proposed in [16]. The method combines the rainfall rate and specific rain attenuation data to arrive at the following equation:

$$r = \frac{\int_0^{D_{\max}} G(D) \exp(-\Lambda D) dD}{\int_0^{D_{\max}} H(D) \exp(-\Lambda D) dD} \tag{8}$$

**Table 1. Input of Simulated DSD and the Output of the Current Method**

Name	R	Input		Output			
		$N_0$	$\Lambda$	$N_0$	$\Lambda$	$ r_{\text{cal}} - r_{\text{meas}} $	$i^{\text{th}}$ iteration
DSD1	$R < 1$	790	3.18	790	3.18	0	219
DSD2	$1 \leq R \leq 2$	1496	2.94	1496	2.94	$7 \times 10^{-18}$	195
DSD3	$2 \leq R \leq 5$	2266	2.66	2266	2.66	$7 \times 10^{-18}$	167
DSD4	$5 \leq R \leq 10$	3291	2.41	3291	2.41	$7 \times 10^{-18}$	142
DSD5	$10 \leq R \leq 20$	7850	2.47	7850	2.47	$7 \times 10^{-18}$	148

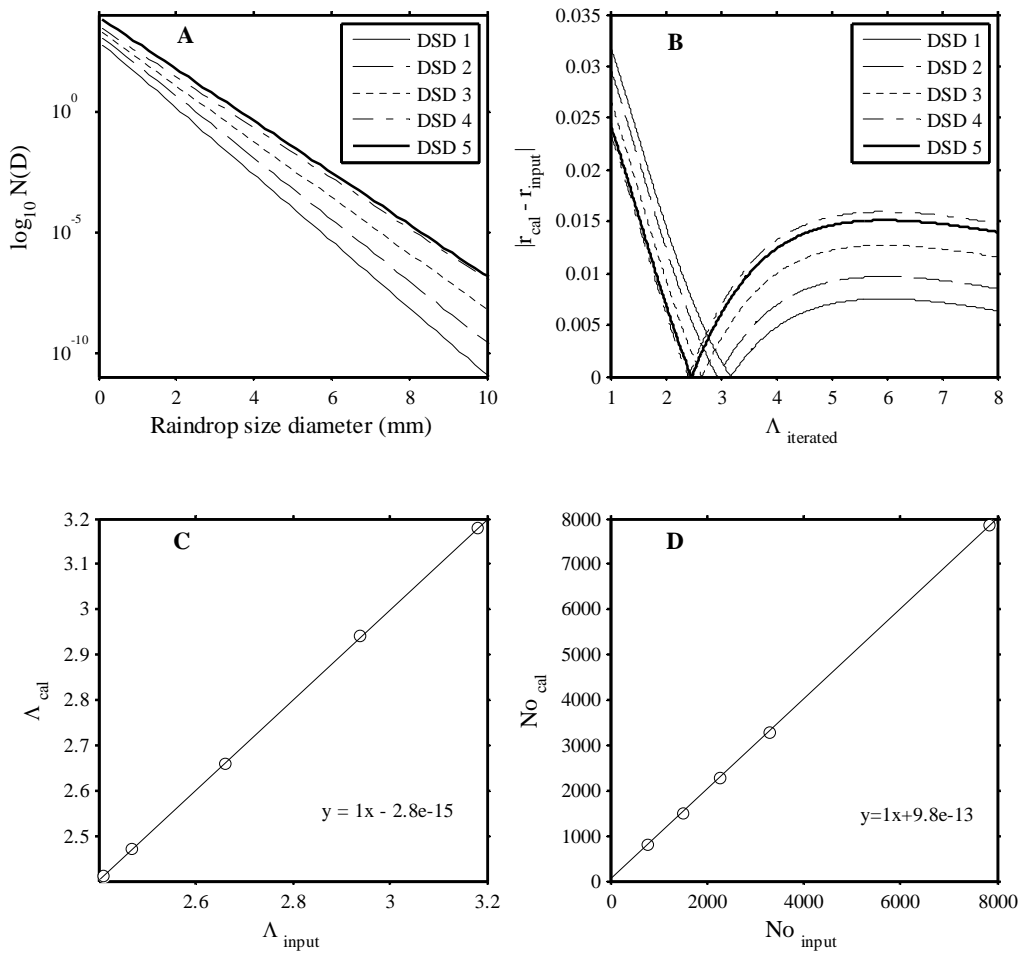


**Figure 1.** (a) Simulated DSD from the Parameters in Tokay et al. [25], (b) Variation of  $|r_{\text{cal}} - r_{\text{input}}|$  for Different Values of  $\Lambda$  iterated from 1-8 with the Interval of 0.01, (c) and (d) are Scatter Plot of Calculated  $\Lambda$  and  $N_0$  versus the Initial or Input Value

Where  $G(D)$  and  $H(D)$  are given by

$$G(D) = 4.343 \times 10^3 \sigma_{ext}(D) \tag{9}$$

$$H(D) = 6 \times 10^{-4} v(D) D^3 \tag{10}$$

The division of  $\gamma$  by  $R$  results in the elimination of  $N_0$  from equation (2). Therefore, the final form of the equation is only a function of  $\Lambda$  (equation 8) and the rest of the quantities (equations 9-10) can be calculated. The left part of equation (8) stems from the measurement, while the right part stems from the calculation. The value of  $\Lambda$  can easily be calculated via an iterative procedure to minimize the residual of  $r_{measured} - r_{calculated}$  in equation (8). The iteration is conducted in the range of  $\Lambda=1-8$ , with an interval of 0.01. Such a range of iteration is selected based on the existing  $\Lambda$  value from the disdrometer measurement [1]. Once the parameter  $\Lambda$  is obtained,  $N_0$  can be calculated by substituting  $\Lambda$  into equations (3) or (5).

The validation of the method is important because the DSD parameters in nature are inherently unknown. Therefore, prior to analyzing the measured data, the method is first employed on simulated data. The DSD parameters in [25] are used to simulate the DSD (Table 1 and Figure 1a), rainfall rate, and specific rain attenuation data. The ability of the method to recover the parameters of known DSDs from which the samples were taken is very good, which is indicated by the high correlation between the input and calculated parameters (Table 1 and Figures 1c-d). It can also be seen that the best  $\Lambda$  can be obtained simply by taking the smallest  $r_{calculated} - r_{input}$  among all the iteration steps (Figure 1b). The second validation method is to compare the DSD parameters obtained from the specific rain attenuation data with those estimated from the 2D video disdrometer (2DVD) data. The 2DVD is an optical instrument used to measure the shape, size, and falling velocity of raindrops. A description and analysis of the performance of the 2DVD at Koto Tabang can be found in [8]. The DSD parameters from the 2DVD data are calculated by following the method proposed by [26].

## Results and Discussion

**Stratiform rain.** Figure 2 shows the time sequential records for the attenuation of the telecommunications satellite Ku-band frequency (12.3992 GHz) as well as the point rain rate for a typical rainfall event on March 27, 2006. Stratiform systems are characterized by relatively weak vertical velocity fields, lower rainfall intensity, and greater horizontal homogeneity [21]. Moreover, the duration of this rain type is more than 1 hour, which can be clearly seen for the case of March 27 (04:36-07:36 Local Time (LT)). The maximum rainfall

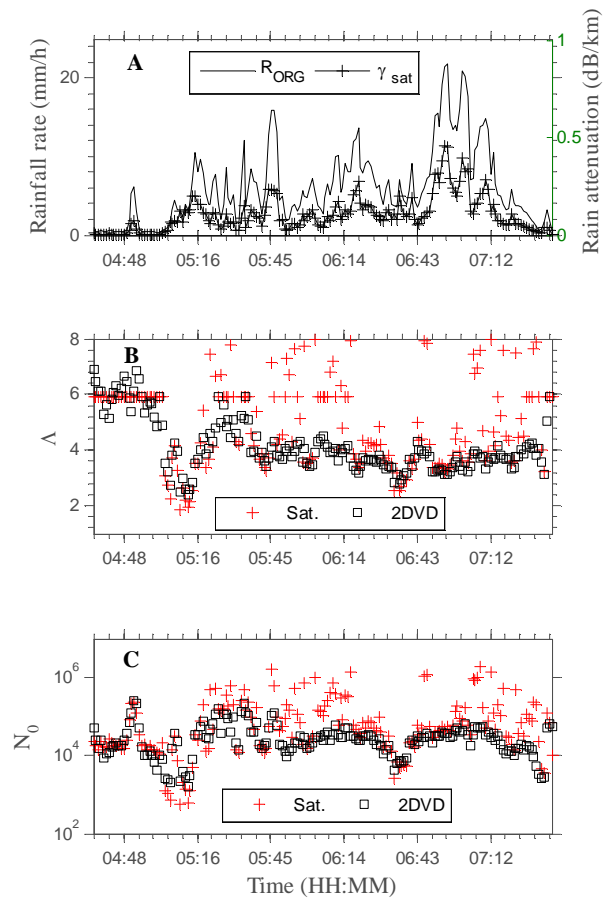


**Figure 2. Rainfall Rate from the ORG and Specific Rain Attenuation of Down-link Radio Wave Signals of Satellite Superbird C (a),  $\Lambda$  (b) and  $N_0$  (c) Calculated from the Specific Rain Attenuation and 2DVD, for Stratiform Rain Event on March 27, 2006**

intensity is observed as approximately 22 mm/h at 6:55 LT, with the specific rain attenuation of 0.45 dB/km. The specific rain attenuation was calculated using a propagation path length of 5 km [20].

Figures 2b-c show a comparison of the DSD parameters obtained using the satellite data and those estimated from the 2DVD data. Some portions of the time series show a good agreement between the DSD parameters of the two data sources. However, a significant difference in the parameters obtained from the satellite and the 2DVD can also be observed. Linear regression between  $\Lambda_{Sat}$  and  $\Lambda_{2DVD}$  has the regression equation of  $y = 0.39x + 2.26$ , with a coefficient ( $r^2$ ) of 0.56. Moreover, the regression coefficient for  $\log_{10}(N_0)$  is  $r^2 = 0.71$ , with the regression equation  $y = 0.41x + 2.43$ . The difference in the DSD parameters ( $\Delta\Lambda$  and  $\Delta N_0$ ) obtained from the satellite and 2DVD data is observed at the beginning rain stage, although it is also clearly observed at the mature stage. The difference occurs not only during

light rain, but also during a high rainfall rate (Figure 3). In general, the parameters derived from the attenuation data are larger than those from the 2DVD data, which is indicated by the positive  $\Delta N_0$  and  $\Delta \Lambda$ .

The second case of stratiform rain is the event of April 20, 2006 (Figure 4a). This is an afternoon rain event with a duration of 3 hours. A maximum rainfall rate of approximately 25 mm/h is observed at 17:47 LT, causing the specific rain attenuation of 0.5 dB/km. Another peak in the rainfall rate (22 mm/h) is observed at 19:04 LT, with the specific rain attenuation of 0.31 dB/km. Although the maximum rainfall intensity of this rain event is higher than that of the March 27 event, its mean rainfall rate is much lower (Table 2). Therefore, with the exception of the two peaks, this second case has a steady rainfall rate. The time series of the DSD parameters obtained using the current method and the 2DVD data is given in Figures 4b-c. In general, the correlations between the parameters obtained from the satellite data and the 2DVD are very good, with  $r^2 \approx 0.9$ .

The performance of the current method is different for the two cases of stratiform rain events (Figures 5). Although the rain type is the same, the DSD parameters of the first case cannot be well retrieved by the current method. This reinforces the findings of previous studies [17] that solutions are not yet available for all sets of experimental observations. Experimental measurements may not be sufficiently accurate to yield a realistic solution, which can occur for two reasons. First, the constant path length assumption may not be as accurate for long duration rain such as stratiform, particularly when the fluctuation of rain intensity is high, as it was in the first case. The evolution of a precipitation system will result in different rain top heights and horizontal

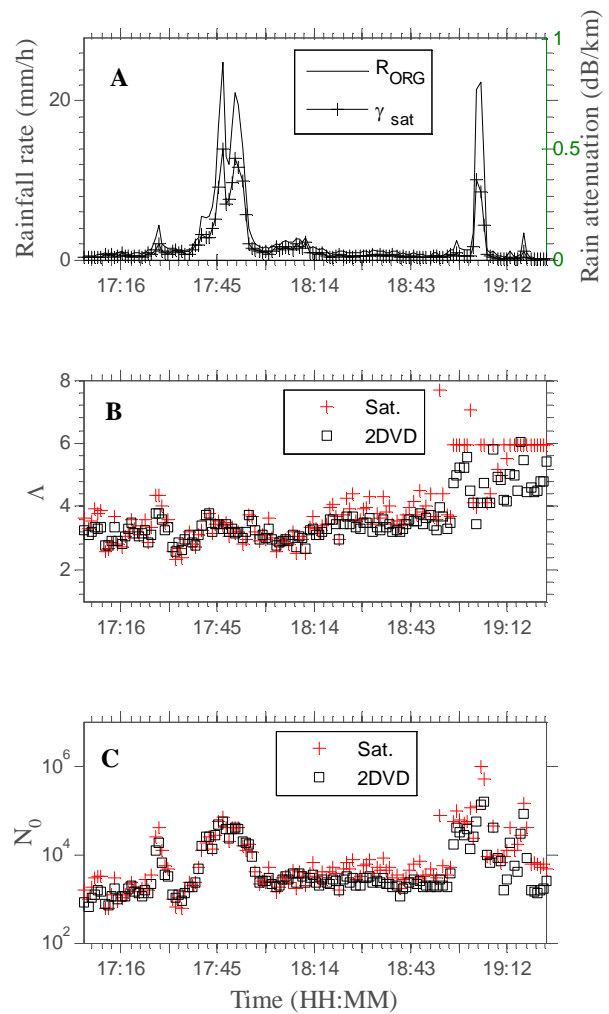


Figure 4. Same as Figure 2, but for Stratiform Rain Event on April 20, 2006

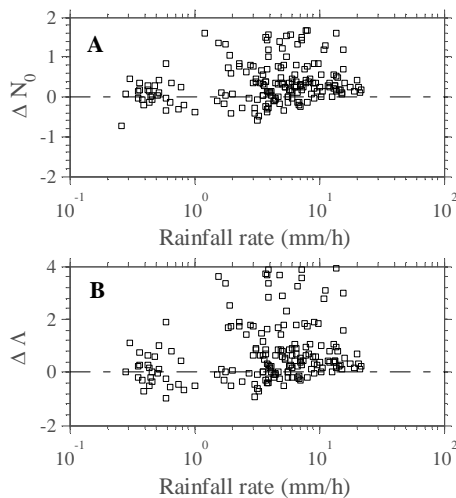


Figure 3. Value of  $\Delta N_0$  ( $N_{0sat} - N_{02DVD}$ ) and  $\Delta \Lambda$  ( $\Lambda_{sat} - \Lambda_{2DVD}$ ) versus Rainfall Rate for Stratiform Rain Event on March 27, 2006

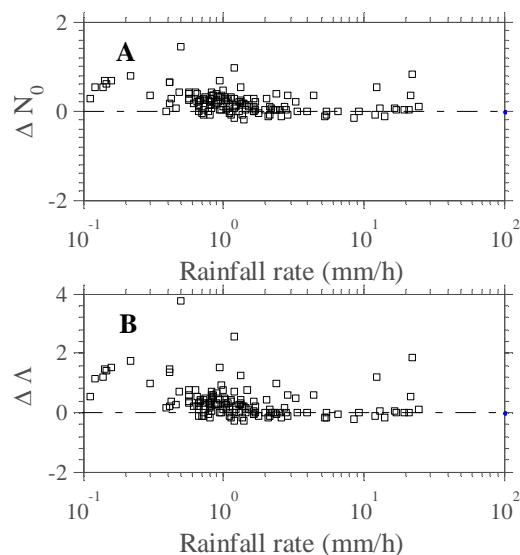
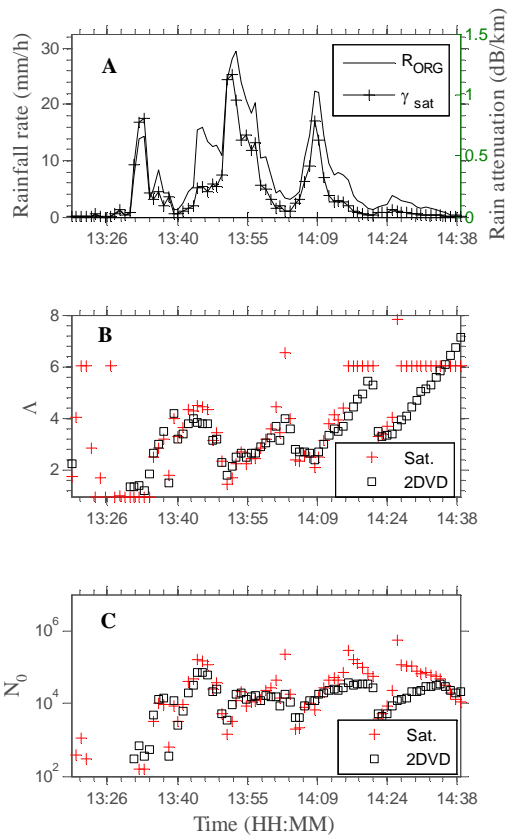


Figure 5. Same as Figure 3, but for Stratiform Rain Event on April 20, 2006

**Table 2. Statistics of Selected Rain Event**

Event	Type	Temperature (°C)		Rainfall rate (mm/h)		
		Mean	Std	Mean	Std	Max.
March 27, 2006 (04: 36-07: 36 LT)	Stratiform	18.72	0.45	5.96	4.81	21.79
April 20, 2006 (17:06-19:24 LT)	Stratiform	20.00	0.00	2.74	4.74	24.85
Sept. 5, 2006 (13: 00-15: 00 LT)	Deep conv.	21.56	1.44	6.72	7.41	25.61
Sept. 7, 2006 (16: 28-17: 20 LT)	Deep conv.	21.39	1.44	31.91	31.75	106.18
March 9, 2006 (15:54-17:34 LT)	Shallow conv.	21.26	0.90	12.30	16.10	82.80
April 21, 2006 (14:58-16:58 LT)	Shallow conv.	20.07	0.25	8.60	8.54	51.54



**Figure 6. Same as Figure 2, but for Deep Convective Rain Event on September 5, 2006**

homogeneity for each stage of the rain. Therefore, a constant path length assumption throughout the rain may not be acceptable. If the experimental measurements are sufficiently accurate, the relatively poor performance of the method was observed at a low rainfall rate [17]. Thus, when attenuations are small and the accuracy of the attenuation measurements is lower, experimental measurements may not be sufficiently accurate, and so the solutions are mostly unrealistic. Although the number of iterations is increased, the value of  $|r_{\text{calculated}} - r_{\text{measured}}|$  remains high ( $> 10^{-4}$ ).

**Deep convective rain.** Figure 6a shows the time series of rain attenuation and the point rain rate for a typical

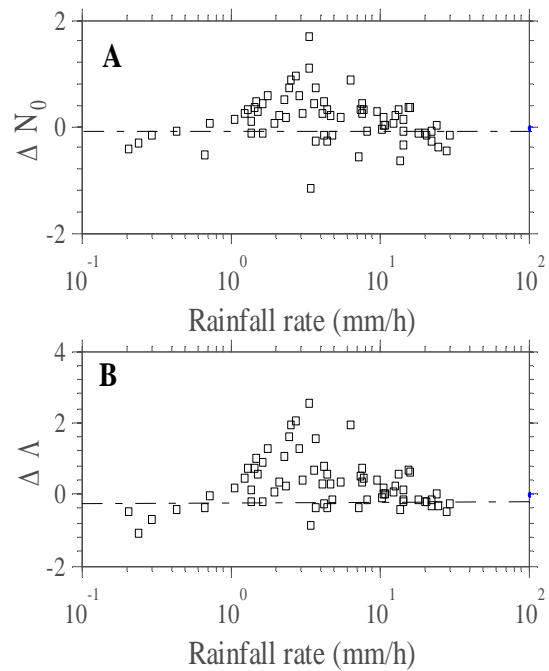


**Figure 7. Same as Figure 3, but for Deep Convective Rain Event on September 5, 2006**

deep convective rain event on September 5, 2006. Deep convective systems are associated with high rainfall intensities of a short duration, strong vertical velocity fields, and small areal coverage [21]. The duration of the September 5 event is about 1 hour. A maximum rainfall rate of approximately 26 mm/h is observed at 13:53 LT, with the specific attenuation of 0.95 dB/km. Another peak (23 mm/h) is visible at 14:09 LT, with the specific rain attenuation of 0.79 dB/km. The specific attenuation was derived using a propagation path length of 4 km [20]. In general, the correlations between the DSD parameters obtained from the satellite data and the 2DVD are good (Figures 6b-c), with  $r^2 \approx 0.9$ . A slight difference in the DSD parameters is observed at a low rainfall rate ( $R < 5$  mm/h), with the specific attenuation of  $< 0.05$  dB/km (Figure 7).

The rain event of September 7, 2006 is selected as the second case of deep convective rain (Figure 8a). It is an



afternoon rain event lasting for 1 hour (16:28-17:20 LT). The intensity of the rainfall in the second case is very high, with the maximum value exceeding 100 mm/h (16:56 LT) and the specific attenuation of 4.32 dB/km. Another heavy rainfall rate is observed at 16:43 LT, with an intensity of 84 mm/h and the specific attenuation of 3.60 dB/km. The path length for this event was assumed to be 4 km [20]. As in the first case, the DSD parameters from the attenuation data show a good agreement with those derived from the 2DVD, with the correlation coefficients for  $\Lambda$  and  $N_0$  being 0.91 and 0.76, respectively. A slight difference is observed during several minutes following 17:05 LT. The rain intensity during this period is so low that the accuracy of the attenuation measurements may be low. Consequently, the solution for the DSD parameters is either not obtainable or unrealistic.

A good overall agreement is found between the DSD parameters obtained from the attenuation and the 2DVD for the two cases of deep convective rains. This may indicate that a constant path length assumption in cases of deep convective rain is acceptable. The propagation path length is influenced by the precipitation height and the coverage area. Different from stratiform rain, the

duration of deep convective rain is short. Therefore, the change in precipitation height and coverage area during deep convective rain may not be significant. These two cases also reinforce the notion that the DSD parameters are either not obtainable or unrealistic when the accuracy of the attenuation measurements is low (at low rainfall rate) (Figure 9), as observed in the stratiform case.

**Shallow convective rains.** Figure 10 shows the time sequential records for the attenuation and rainfall rate of a typical shallow convective rain event on March 9, 2006. The duration of this event is approximately 1.5 hours (15:54-17:34 LT). The maximum rainfall intensity of 83 mm/h is observed at 16:34 LT, with the specific rain attenuation of 4.50 dB/km. Another high rainfall rate of 57 mm/h is seen at 16:20 LT, with the specific attenuation of 2.94 dB/km. Shallow convective rain is formed from warm processes, so it has hydrometeors confined entirely below the melting level [21]. Therefore, the rain top height of shallow convective rain is lower than the melting level (< 5 km). Consequently, the propagation path length of this rain type is much shorter than that of deep and shallow convective rains. For the case of March 9, the path length was assumed to be 2 km [20].

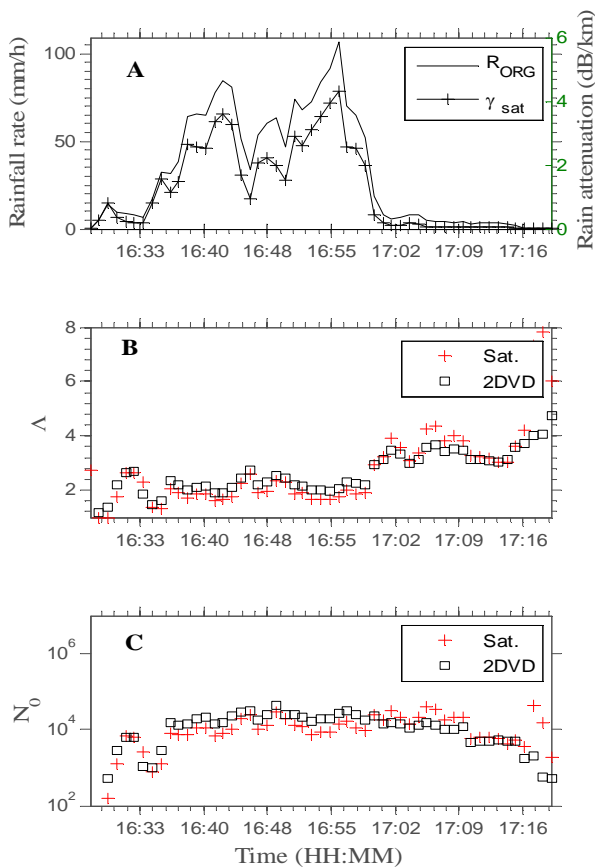


**Figure 8.** Same as Figure 2, but for Deep Convective Rain Event on September 7, 2006

Figures 10b-c show a comparison of the DSD parameters obtained using the attenuation of satellite data and those estimated from the 2DVD. The parameters obtained from the satellite data are in good agreement with those obtained from the 2DVD, with the regression coefficients being 0.95 and 0.88 for  $\Lambda$  and  $N_0$ , respectively. As in the previous cases, the difference between the DSD parameters obtained from the satellite data and the 2DVD is observed at light rain (after 17:06 LT) and can also be seen from Figure 11. The second case of shallow convective rain is the event of April 21, 2006 (Figure 12a), with a duration of 2 hours. A maximum rainfall rate of 52 mm/h is observed at 15:48 LT, causing the specific rain attenuation of 0.98 dB/km. Another peak in the rainfall rate (34 mm/h) is observed at 15:38 LT, with the specific rain attenuation of 0.5 dB/km. As in the first case of shallow convective rain, the specific attenuation was also derived using a propagation path length of 2 km [20]. The time series of the DSD parameters obtained using the current method and the 2DVD data is given in Figures 12b-c. It can be clearly seen that the method cannot retrieve the DSD parameters for this case. The regression coefficient between the parameters obtained from the satellite data and the 2DVD is very low (i.e.,  $r^2 \approx 0.27$ ). This may be due to the experimental measurements not being sufficiently accurate to yield a realistic solution. The method cannot achieve the convergence criteria ( $<10^{-5}$ ) in which the value of  $|r_{\text{count}} - r_{\text{measuring}}|$  is high ( $>10^{-4}$ ) throughout the rain. Consequently, the value of  $\Delta$  for this case is high for all intensities (Figure 13).

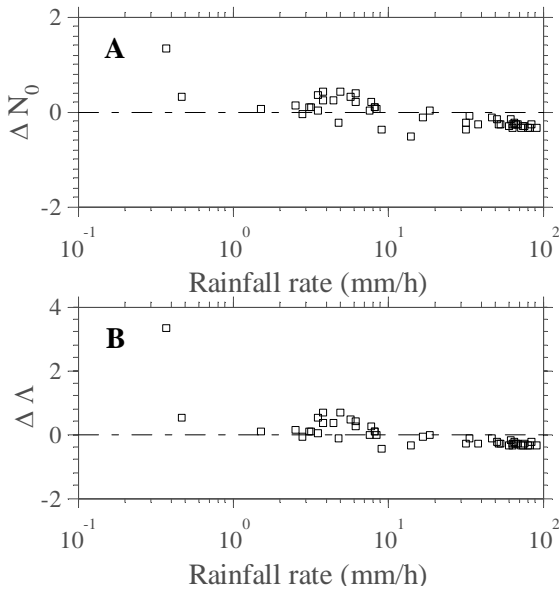


Figure 9. Same as Figure 3, but for Deep Convective Rain Event on September 7, 2006

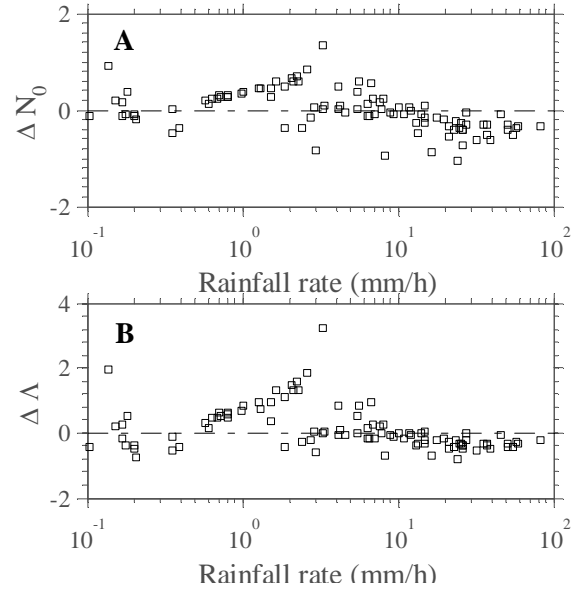


Figure 11. Same as Figure 3, but for Shallow Convective Rain Event on March 9, 2006

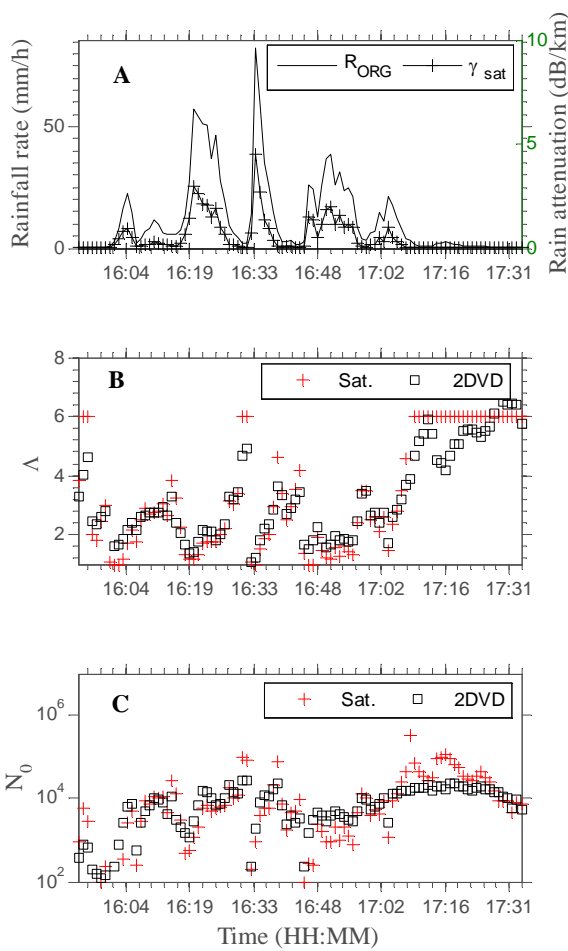


Figure 10. Same as Figure 2, but for Shallow Convective Rain Event on March 9, 2006

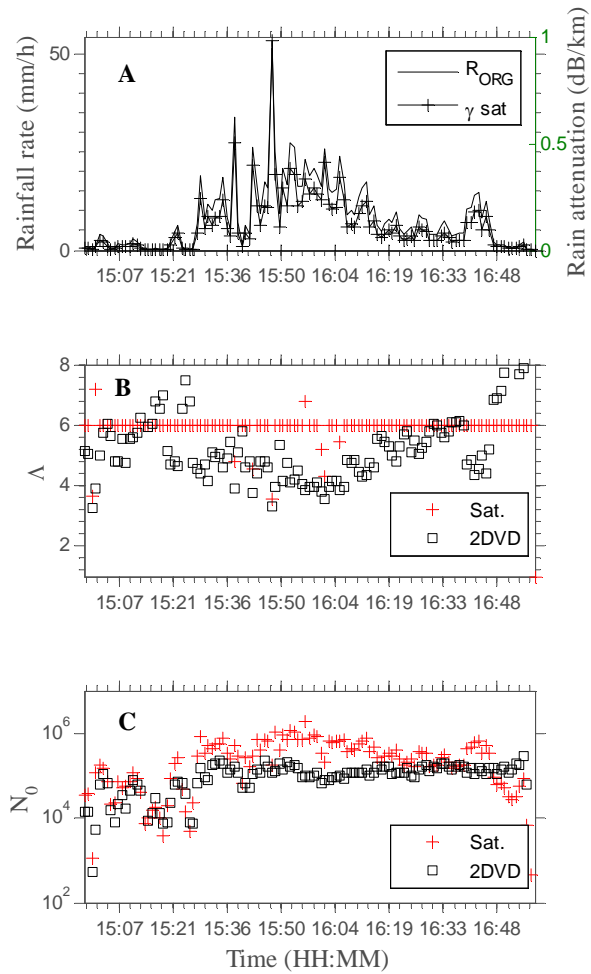
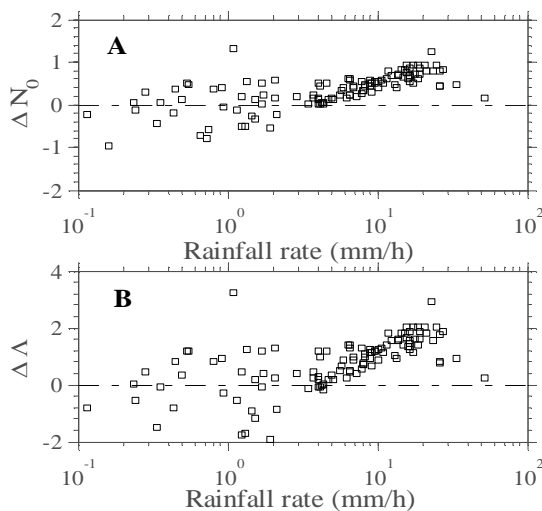


Figure 12. Same as Figure 2, but for Shallow Convective Rain Event on April 21, 2006



**Figure 13.** Same as Figure 3, but for Shallow Convective Rain Event on April 21, 2006

## Conclusions

The results presented in this paper serve to roughly quantify the possibility of estimating the DSD parameters by combining the point rain rate and the specific rain attenuation of a Ku-band communications satellite. The method was examined for two case studies of stratiform rain and two case studies of deep and shallow convective rain. The DSD parameters of deep convective rains with a short duration and stratiform rains with stable rain intensity can be retrieved by this method with only a small error rate in comparison to the 2DVD. The low rainfall rate associated with low rain attenuation means that the accuracy of the attenuation measurements may be insufficient, so that the solutions are mostly unrealistic. For shallow convective rain, the accuracy of the method is lower than that for stratiform and deep convective rains. It seems that the constant propagation path length assumption of 2 km may not always be acceptable for all shallow convective rains or throughout the rain event. Thus, the accuracy of the current method may increase when the bias in estimating the specific rain attenuation can be reduced. The path length assumption for each rain type needs to be studied in more detail in the future, which will involve more datasets. Despite the above limitations, satellite communication data can be utilized to estimate the DSD parameters, particularly when an instrument that directly measures the DSD is not available.

## Acknowledgments

The authors wish to thank Prof. Maekawa Yasuyuki and Prof. Yoshiaki Shibagaki (Osaka Electro-Communication University) for providing the data concerning the down-link radio wave signals of the Superbird-C satellite. We also wish to thank Dr. Hiroyuki Hashiguchi (Kyoto

University), Dr. Toyoshi Shimomai, and Prof. Toshiaki Kozu (Shimane University) for their assistance in the collection and processing of the 2DVD and ORG data. The 2DVD and other Equatorial Atmospheric Radar (EAR) facilities at Koto Tabang are supported by Grant-Aid for Scientific Research on Priority Areas, which is funded by the Ministry of Education, Culture, Sports, Science, and Technology (MEXT) of Japan. This study is partially supported by the Faculty of Mathematics and Natural Science of Andalas University under Hibah Mandiri-2013.

## References

- [1] Tokay, A. Short, D.A. 1996. Evidence from tropical raindrop spectra of the origin of rain from stratiform versus convective clouds. *J. Appl. Meteor.* 35: 355-371, [http://dx.doi.org/10.1175/1520-0450\(1996\)035<0355:EFTRSO>2.0.CO;2](http://dx.doi.org/10.1175/1520-0450(1996)035<0355:EFTRSO>2.0.CO;2).
- [2] Cataneo, R. 1969. A method for estimating rainfall rate-radar reflectivity relationships. *J. Appl. Meteor.* 8: 815-819, [http://dx.doi.org/10.1175/1520-0450\(1969\)008<0815:AMFERR>2.0.CO;2](http://dx.doi.org/10.1175/1520-0450(1969)008<0815:AMFERR>2.0.CO;2).
- [3] Kozu, T., Reddy, K.K., Mori, S., Thurai, M., Ong, J.T., Rao, D.N., Shimomai, T. 2006. Seasonal and diurnal variations of raindrop size distribution in Asian monsoon region. *J. Meteorol. Soc. Japan.* 84A: 195-209, <http://doi.org/10.2151/jmsj.84A.195>.
- [4] Marzuki, M., Kozu, T., Shimomai, T., Randeu, W. L., Hashiguchi, H., Shibagaki, Y. 2009. Diurnal variation of rain attenuation obtained from measurement of raindrop size distribution in equatorial Indonesia. *IEEE Trans. Ant. Propag.* 57(4): 1191-1196, doi: 10.1109/TAP.2009.2015812.
- [5] Das, S., Maitra, A., Shukla, A.K. 2010. Rain attenuation modeling in the 10-100 GHz frequency using drop size distributions for different climatic zones in tropical India. *Prog. Electromagn. Res. B.* 25: 211-224, doi: 10.2528/PIERB10072707.
- [6] Coppens, D., Haddad, Z.S., Im, E. 2000. Estimating the uncertainty in passive-microwave rain retrievals. *J. Atmos. Oceanic Technol.* 17: 1618-1629, [http://dx.doi.org/10.1175/1520-0426\(2000\)017<1618:ETUIPM>2.0.CO;2](http://dx.doi.org/10.1175/1520-0426(2000)017<1618:ETUIPM>2.0.CO;2).
- [7] Schönhuber, M., Lammer, G., Randeu, W.L. 2008. The 2-D-Video-Disdrometer. In Michaelides, S. (eds.), *Precipitation: Advances in Measurement, Estimation and Prediction*. Springer. Berlin. pp. 3-31.
- [8] Marzuki, Randeu, W.L. Kozu, T., Shimomai, T., Hashiguchi, H., Schönhuber, M. 2013. Raindrop axis ratios, fall velocities and size distribution over Sumatera from 2D-Video Disdrometer measurement. *Atmos. Res.* 119: 23-37, <http://dx.doi.org/10.1016/j.atmosres.2011.08.006>.
- [9] Sheppard, B.E., Joe, P.I. 2008. Performance of the precipitation occurrence sensor system as a

- precipitation gauge. *J. Atmos. Oceanic Technol.* 25: 196-212, <http://dx.doi.org/10.1175/2007JTECHA957.1>.
- [10] Peters, G., Fischer, B., Münster, H., Clemens, M., Wagner, A. 2005: Profiles of raindrop size distributions as retrieved by Microrain Radars. *J. Appl. Meteor.* 44: 1930-1949, <http://dx.doi.org/10.1175/JAM2316.1>.
- [11] Wakasugi, K., Mizutani, A., Matsuo, M., Fukao, S., Kato, S. 1986. A direct method for deriving drop-size distribution and vertical air velocities from VHF doppler radar spectra. *J. Atmos. Oceanic Technol.* 3: 623-629, [http://dx.doi.org/10.1175/1520-0426\(1986\)003<0623:ADMFDD>2.0.CO;2](http://dx.doi.org/10.1175/1520-0426(1986)003<0623:ADMFDD>2.0.CO;2).
- [12] Yoshikawa, E., Chandrasekar, V., Ushio, T. 2014. Raindrop size distribution (DSD) retrieval for X-band dual-polarization radar. *J. Atmos. Oceanic Technol.* 31(2): 387-403, <http://dx.doi.org/10.1175/JTECH-D-12-00248.1>.
- [13] Oguchi, T. 1983. Electromagnetic wave propagation and scattering in rain and other hydrometeors. *Proc. IEEE*, 71 (9):1029-1078, doi: 10.1109/PROC.1983.12724.
- [14] Bringi, V.N., Chandrasekar, V. 2001. *Polarimetric Doppler Weather Radar: Principles and Applications*. Cambridge University. United Kingdom. pp. 534-569.
- [15] Bohren, C.F., Huffman, D.R. 1983. *Absorption and Scattering of Light by Small Particle*, John Wiley & Sons. Inc. Kanada. pp. 3-222.
- [16] Manabe, T., Ihara, T., Furuhashi, Y. 1984. Inference of raindrop size distribution from attenuation and rain rate measurements. *IEEE Trans. Ant. Propag.* 32(5): 474-478, doi: 10.1109/TAP.1984.1143361.
- [17] Maitra, A., Gibbins, C.J. 1999. Modeling of raindrop size distributions from multiwavelength rain attenuation measurements. *Radio Sci.* 34(3): 657-666, doi: 10.1029/1998RS900045.
- [18] Maekawa, Y., Fujiwara, T., Shibagaki, Y., Sato, T., Yamamoto, M., Hashiguchi, H., Fukao, S. 2006. Effects of tropical rainfall to the Ku-band satellite communication links at the equatorial atmosphere radar observatory. *J. Meteorol. Soc. Jpn.* 84A: 211-225, <http://doi.org/10.2151/jmsj.84A.211>.
- [19] Nystuen, J.A. 1999. Relative performance of automatic rain gauges under different rainfall conditions. *J. Atmos. Oceanic Technol.* 16 (8): 1025-1043, [http://dx.doi.org/10.1175/1520-0426\(1999\)016<1025:RPOARG>2.0.CO;2](http://dx.doi.org/10.1175/1520-0426(1999)016<1025:RPOARG>2.0.CO;2).
- [20] Marzuki. 2011. *Tropospheric Precipitation Microstructure and Its Influence on Electromagnetic Wave Propagation*. Doctoral thesis. Submitted to Institute for Broadband Communication. Graz University of Technology, Austria.
- [21] Williams, C.R., Warner, L.E., Kenneth, S.G. 1995. Classification of precipitating clouds in the tropics using 915-MHz wind profilers. *J. Atmos. Oceanic Technol.* 12: 996-1012, [http://dx.doi.org/10.1175/1520-0426\(1995\)012<0996:COPCIT>2.0.CO;2](http://dx.doi.org/10.1175/1520-0426(1995)012<0996:COPCIT>2.0.CO;2).
- [22] Marshall, J.S., Palmer, W.M. 1948. The Distribution of raindrops with size. *J. Meteorol.* 5:165-166, [http://dx.doi.org/10.1175/1520-0469\(1948\)005<0165:TDORWS>2.0.CO;2](http://dx.doi.org/10.1175/1520-0469(1948)005<0165:TDORWS>2.0.CO;2).
- [23] Atlas, D., Srivastava, R.C., Sekhon, R.S. 1973. Doppler radar characteristics of precipitation at vertical incidence. *Rev. Geophys. Space Phys.* 11(1): 1-35, doi: 10.1029/RG011i001p00001.
- [24] Liebe, H.J., Hufford, G.A., Manabe, T. 1991. A model for the complex permittivity of water at frequencies below 1 THz. *Int. J. Infrared Millimeter Waves.* 12(7): 659-657, doi: 10.1007/BF01008897.
- [25] Tokay, A., Kruger, A. and Krajewski, W.F. 2001. Comparison of drop size distribution measurements by impact and optical disdrometers. *J. Appl. Meteor.* 40: 2083-2097, [http://dx.doi.org/10.1175/1520-0450\(2001\)040<2083:CODSDM>2.0.CO;2](http://dx.doi.org/10.1175/1520-0450(2001)040<2083:CODSDM>2.0.CO;2).
- [26] Waldvogel, A. 1974. The No jump of raindrop spectra. *J. Atmos. Sci.* 31: 1067-1078, [http://dx.doi.org/10.1175/1520-0469\(1974\)031<1067:TJORS>2.0.CO;2](http://dx.doi.org/10.1175/1520-0469(1974)031<1067:TJORS>2.0.CO;2).